SCIENCE CHINA
Information Sciences

• LETTER •

March 2025, Vol. 68, Iss. 3, 139401:1–139401:2
https://doi.org/10.1007/s11432-024-4255-5

# 24.4 THz·V $f_T$×BV figure-of-merit AlN/GaN/AlN MISHEMTs with thin AlN buffer layer

Chaoqun ZHANG[1], Hong ZHOU[1,2*], Sami ALGHAMDI[3], Kun ZHANG[1], Zhihong LIU[1,2], Yue HAO[1] & Jingcheng ZHANG[1*]

[1]*State Key Laboratory of Wide-Bandgap Semiconductor Devices and Integrated Technology, Xidian University, Xi'an 710071, China*
[2]*Guangzhou Wide Bandgap Semiconductor Innovation Center, Guangzhou Institute of Technology, Xidian University, Guangzhou 510555, China*
[3]*Electrical and Computer Engineering Department, King Abdulaziz University, Jeddah 21589, Saudi Arabia*

Received 29 July 2024/Revised 13 October 2024/Accepted 16 December 2024/Published online 11 February 2025

**Citation** Zhang C Q, Zhou H, Alghamdi S, et al. 24.4 THz·V $f_T$×BV figure-of-merit AlN/GaN/AlN MISHEMTs with thin AlN buffer layer. Sci China Inf Sci, 2025, 68(3): 139401, https://doi.org/10.1007/s11432-024-4255-5

Gallium nitride-based high-electron-mobility-transistors (HEMTs) have gained widespread interest and become primary candidates for next-generation high-frequency and high-power RF electronics, due to their wide bandgap, high breakdown field, and strong polarization-induced high-density 2-dimensional electron gas (2DEG) at the hetero-junction interface. AlGaN-based barriers and GaN-based buffers have become the dominant commercialized device structures for radar, satellite, and 5G communications [1,2]. In order to further improve device performances in terms of frequency and power, AlN barrier and buffer are generally proposed. The AlN-based platform is favored due to its ultra-wide bandgap (UWB) properties, which include a strong polarization capability, resulting in higher 2DEG density and increased saturation current. Additionally, AlN's high critical electric field contributes to a higher breakdown voltage (BV), and its excellent thermal conductivity offers enhanced heat dissipation. These characteristics significantly enhance the quantum confinement effects in HEMT, thereby improving the direct current (DC) and radio frequency (RF) performance of the device [3, 4]. The primary challenge in utilizing AlN-based HEMTs lies in the difficulty of growing high-quality AlN. The quality here is particularly focused on achieving low defect density, high BV, and low leakage current, which are critical parameters for the optimal performance of HEMT.

In this study, we propose an MOCVD-grown SiN/AlN/GaN/AlN/SiC epitaxial wafer to boost the $f_T$×BV performance for next-generation GaN RF power transistors. With a thin AlN buffer layer, GaN MISHEMT achieves a high BV of 214 V at $L_{GD}$ = 1.7 μm and $L_G$ = 100 nm. Combining a $f_T$ = 114 GHz, a record $f_T$×BV JFOM of 24.4 THz·V is demonstrated. Along with a high $I_D$ of 2.5–3.1 A/mm, and a high $g_m$ of 0.5–0.7 S/mm. GaN MISHEMTs with the AlN platform verify their great promise for next-generation millimeter wave high-power applications.

*Experiments.* The cross-sectional schematic image and scanning electron microscopy (SEM) image of the fabricated rectangular-gate devices are shown in Figures 1(a) and (b). The AlN/GaN/AlN MISHEMT epi-layers were grown on a 4-inch SiC substrate by MOCVD. The sheet resistance, carrier density and electron mobility are measured to be 220 Ω/□, $2.3\times10^{13}$/cm$^2$ and 1280 cm$^2$/V·s, respectively, from Hall measurements. The manufacturing process starts with mesa isolation with dry etching. Then, Ti/Al/Ni/Au based alloyed Ohmic contact was deposited above the SiN layer and followed by 875°C rapid thermal annealing under $N_2$ ambient, the $R_C$ is extracted to be around 0.3 Ω·mm from the transfer length method. Rectangular gates with $L_G$ of 100 nm are formed by electron-beam lithography and followed by Ni/Au deposition. The devices are with source (S) to drain (D) spacings ($L_{SD}$) of 0.7–2.3 μm. For the sub-micron $L_{SD}$ (0.7 μm) device, the gate electrode is positioned centrally between the source and drain. For larger $L_{SD}$ devices, the gate is located approximately 500 nm away from the source.

*Results and discussion.* Representative direct-current output characteristics ($I_D$-$V_{SD}$) of AlN/GaN/AlN MISHEMTs with $L_G$ = 100 nm, $L_{SD}$ = 0.7 and 2.3 μm are plotted in Figures 1(c) and (d). The gate voltage ($V_{GS}$) is biased from 2 to −6 V with −1 V as a step and the $V_{DS}$ is swept from 0 to 10 V. The on-resistance at $V_{GS}$ = 2 V is determined to be 0.8 and 1.1 Ω·mm for $L_{SD}$ 0.7 and 2.3 μm, respectively. A peak $I_D$ of 3.1 and 2.5 A/mm is achieved at $V_{GS}$ = 2 V and $V_{DS}$ = 10 V for $L_{SD}$ = 0.7 and 2.3 μm, respectively. Linear-scale transfer and transconductance ($I_D$-$V_{GS}$-$g_m$) characteristics at $V_{DS}$ = 7 V of those two devices are summarized in Figure 1(e). The peak $g_m$ is determined to be 0.72 and 0.51 S/mm for $L_{SD}$ = 0.7 and 2.3 μm, respectively. The well-behaved log-scale $I_D$-$V_{GS}$-$I_G$ of representative AlN/GaN/AlN MISHEMT with $L_{SD}$ =

* Corresponding author (email: hongzhou@xidian.edu.cn, jchzhang@xidian.edu.cn)

 

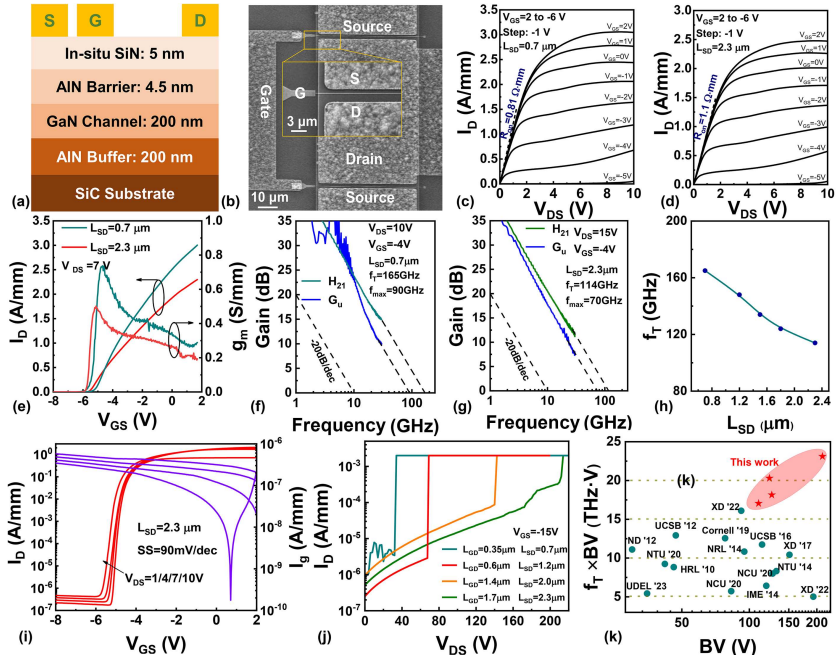


**Figure 1** (Color online) (a) Cross-sectional schematic and (b) SEM image of representative GaN MISHEMT. Direct-current output characteristics of the device with (c) $L_{SD}$ = 0.7 μm and (d) $L_{SD}$ = 2.3 μm. (e) Linear-scale transfer and transconductance characteristics of the same devices. Pad de-embedded small-signal RF characteristics of $L_G$ = 100 nm GaN MISHEMTs with (f) $L_{SD}$ = 0.7 μm and (g) $L_{SD}$ = 2.3 μm. (h) Extracted $f_T$ versus $L_{SD}$ of various GaN MISHEMTs. (i) Log-scale $I_D$-$V_{GS}$-$I_G$ curves of the device with $L_{SD}$ = 2.3 μm. (j) Three-terminal off-state breakdown measurement results of GaN MISHEMTs. (k) BV vs. $f_T$×BV FOM comparisons of state-of-the-art GaN RF transistors.

2.3 μm at $V_{DS}$ = 1/4/7/10 V are summarized in Figure 1(i). The SS is extracted to be 90 mV/dec from 2–3 orders of continuous subthreshold $I_D$. The drain-induced barrier lowering is calculated to be $V$ = 37 mV/V at $I_D$ = 10–4 A/mm. Even with a small $L_G$ = 100 nm, an $I_D$ on/off ratio of $10^7$ is also achieved. Three terminal off-state breakdown measurement results at $V_{GS}$ = −15 V for various $L_{GD}$ from 0.3 to 1.7 μm are summarized in Figure 1(j). Even without a field-plate design, the device with $L_{GD}$ = 1.7 μm achieves a high BV = 214 V. By increasing the $L_{GD}$, the BV can be essentially enhanced. Compared with some previous results with thick GaN buffer layers, the BV is only measured to be 50 V for an $L_{GD}$ = 1 μm. The significantly enhanced BV is most likely caused by the UWB nature of AlN and better quantum confinement, especially for those deep sub-micron $L_G$. The averaged breakdown field is fitted to be 1.2 MV/cm, which is around 2–3 times that of GaN HEMTs with GaN buffer. The variation of the leakage current at $V_{DS}$ = 0 V is most likely related to the nonuniformity of the mesa isolation etching process induced surface damage. Small signal RF performances of AlN/GaN/AlN MISHEMTs with $L_{SD}$ = 0.7 and 2.3 μm are shown in Figures 1(f) and (g) at $L_G$ = 100 nm. The $f_T$ and $f_{max}$ are determined by a conservative −20 dB/dec extrapolation methodology from low-frequency regions. Only the open structure without conductive mesa is used for parasitic de-embedding. An $f_T/f_{max}$ of 114/60 and 165/90 GHz are extracted for $L_{SD}$ = 2.3 and 0.7 μm, respectively. The $f_T$ dependence on the $L_{SD}$ is exhibited in Figure 1(h). By increasing the $L_{SD}$, the $f_T$ is slowly reduced. Combing with the high BV, a maximum $f_T$×BV FOM of 114 GHz × 214 V = 24.4 THz·V is demonstrated, which is one of the highest values among all state-of-the-art GaN RF power transistors, as compared in Figure 1(k) [5,6].

*Conclusion.* In this study, we have shown that AlN/GaN/AlN MISHEMTs on an MOCVD-grown GaN epi-wafer with thin AlN buffer can substantially achieve a state-of-the-art $f_T$×BV JFOM of 24.4 THz·V. This thin AlN buffer layer can provide better quantum confinement and the UWB nature induced high critical field are two essential factors for the enhanced BV of GaN RF power transistors. Combined with an AlN barrier, the MISHEMTs achieve high $I_D$, $g_m$, and $f_T$ simultaneously. This performance validates the significant potential of the proposed AlN/GaN/AlN MISHEMT for high-frequency, high-output power, and high-efficiency RF devices, essential for next-generation high-power millimeter-wave RF systems.

**Acknowledgements** This work was supported by National Key Research and Development Program of China (Grant No. 2021YFA0716400) and National Natural Science Foundation of China (Grant No. 62222407).

**References**

1 Romanczyk B, Wienecke S, Guidry M, et al. Demonstration of constant 8 W/mm power density at 10, 30, and 94 GHz in state-of-the-art millimeter-wave N-polar GaN MISHEMTs. IEEE Trans Electron Devices, 2018, 65: 45–50
2 Hickman A, Chaudhuri R, Li L, et al. First RF power operation of AlN/GaN/AlN HEMTs with > 3 A/mm and 3 W/mm at 10 GHz. IEEE J Electron Devices Soc, 2021, 9: 121–124
3 Hickman A, Chaudhuri R, Bader S J, et al. High breakdown voltage in RF AlN/GaN/AlN quantum well HEMTs. IEEE Electron Dev Lett, 2019, 40: 1293–1296
4 Moon J S, Grabar B, Wong J, et al. W-band graded-channel GaN HEMTs with record 45% power-added-efficiency at 94 GHz. IEEE Microw Wireless Tech Lett, 2023, 33: 161–164
5 Yang L, Jia F, Lu H, et al. Record power performance of 33.1 W/mm with 62.9 PAE at X-band and 14.4 W/mm at Ka-band from AlGaN/GaN/AlN:Fe heterostucture. In: Proceedings of International Electron Devices Meeting (IEDM), 2023. 1–4
6 Wang P F, Mi M H, Zhang M, et al. Demonstration of 16 THz V Johnson's figure-of-merit and 36 THz V $f_{max}$·$V_{BK}$ in ultrathin barrier AlGaN/GaN HEMTs with slant-field-plate T-gates. Appl Phys Lett, 2022, 120: 102103